Mon. Not. R. Astron. Soc. **298,** 777–789 (1998)

Systematic construction of exact magnetohydrodynamic models for astrophysical winds and jets

N. Vlahakis[1⋆] and K. Tsinganos[1,2⋆]
[1]*Department of Physics, University of Crete, GR-710 03 Heraklion, Crete, Greece*
[2]*Foundation for Research and Technology Hellas (FORTH), GR-711 10 Heraklion, Crete, Greece*

Accepted 1998 March 18. Received 1998 March 17; in original form 1997 December 30

ABSTRACT

By a systematic method we construct general classes of exact and self-consistent axisymmetric magnetohydrodynamic (MHD) solutions describing flows that originate in the near environment of a central gravitating astrophysical object. The unifying scheme contains two large groups of exact MHD outflow models: (I) meridionally self-similar models with *spherical* critical surfaces; and (II) radially self-similar models with *conical* critical surfaces. This classification includes known polytropic models, such as the classical Parker description of a stellar wind and the Blandford & Payne model of a disc wind; it also contains non-polytropic models, such as those of winds/jets in Sauty & Tsinganos, Lima, Tsinganos & Priest, and Trussoni, Tsinganos & Sauty. Besides the unification of all known cases under a common scheme, several new classes emerge and some are briefly analysed; they could be explored for a further understanding of the physical properties of MHD outflows from various magnetized and rotating astrophysical objects in stellar or galactic systems.

Key words: MHD – solar wind – stars: atmospheres – stars: mass-loss – ISM: jets and outflows – galaxies: jets.

1 INTRODUCTION

A widespread phenomenon in astrophysics is the outflow of plasma from the environment of stellar or galactic objects, either in the form of a non-collimated wind (Parker 1958; Feldman et al. 1996), or in the form of collimated jets (Blandford & Rees 1974; Biretta 1996). These outflows not only occur around typical stars and the nuclei of many radio galaxies and quasars, but are also associated with young stars, older mass-losing stars and planetary nebula nuclei, symbiotic stars, black hole X-ray transients, low- and high-mass X-ray binaries and cataclysmic variables (for recent reviews see e.g., respectively, Ferrari et al. 1996, Ray 1996, Kafatos 1996, Mirabel & Rodriguez 1996 and Livio 1997). Even for the two spectacular rings seen with the *Hubble Space Telescope* (*HST*) in SN1987A, it has been proposed that they may be produced by two precessing jets from an object similar to SS433 on a hourglass-shaped cavity which is created by non-uniform winds from the progenitor star (Burderi & King 1995; Burrows et al. 1995). Also recently, in the well-known long jet of the distant radio galaxy NGC 6251, an $\sim 10^3$ light-year-wide warped dust disc perpendicular to the main jet axis has been observed by *HST* to surround and reflect UV light from the bright core of the galaxy which probably hosts a black hole (Crane & Vernet 1997).

Nevertheless, despite their abundance, the questions of the formation, acceleration and propagation of non-uniform winds and jets have not been fully resolved. One of the main difficulties in dealing with the theoretical problem posed by cosmical outflows is that their dynamics needs to be described – even to lowest order – by the highly intractable set of magnetohydrodynamic (MHD) equations. As is well known, this is a non-linear system of partial differential equations with several critical points, etc., and only a very few classes of solutions are available for axisymmetric systems obtained by assuming a separation of variables in several key functions. This hypothesis allows an analysis in a 2D geometry of the full MHD equations which reduce then to a system of ordinary differential equations. The basis of such a self-similarity treatment is the prescription of a scaling law in the variables as a function of one of the coordinates. The choice of the scaling variable depends on the specific astrophysical problem.

In spherical coordinates (r, θ, ϕ), a *first* broad class for describing outflows comprises the so-called meridionally self-similar MHD models. Parker's (1958) classical modelling of the spherically symmetric polytropic solar wind is the simplest member of this class. A new class of such a type of model for describing magnetized and rotating MHD outflows from a central gravitating object has also been examined (Sauty & Tsinganos 1994, henceforth ST94; Lima, Tsinganos & Priest 1996; Trussoni, Tsinganos & Sauty 1997). For example, an energetic criterion for the transition of an asymptotically conical outflow originating at an inefficient magnetic rotator to an asymptotically cylindrical outflow from an

⋆E-mail: vlahakis@physics.uch.gr (NV); tsingan@physics.uch.gr (KT)

efficient magnetic rotator was derived. In the present paper, it will be shown that this special class of meridionally self-similar solutions is one of the simplest possible meridionally self-similar models. Furthermore, a new interesting member of this class of radially self-similar MHD models will be briefly sketched.

A *second* broad class of solutions contains the radially self-similar MHD models. Bardeen & Berger (1978) presented the first such models in the context of hydrodynamic and polytropic galactic winds. Nevertheless, their generalization to a cold magnetized plasma by Blandford & Payne (1982, henceforth BP82) remains widely known because of their success in showing for the first time that astrophysical jets can be accelerated magnetocentrifugally from a Keplerian accretion disc, *if* the poloidal fieldlines are inclined by an angle of 60°, or less, to the disc mid-plane (but see also Cao 1997). A further extension has been presented by Contopoulos & Lovelace (1994) for a hot plasma with a more general parametrization of the magnetic flux on the disc, while these models form the basis of several investigations of accretion–ejection flows from stars and active galactic nuclei (AGN) (Konigl 1989; Ferreira & Pelletier 1995; Ferreira 1997; Li 1995). In this paper it will be shown that this special class of radially self-similar solutions is one of the simplest possible such models. Furthermore, a new interesting member of the radially self-similar MHD models will be sketched.

The paper is organized as follows. After a brief introduction of the basic MHD quantities, in Section 2.1 we use a simple theorem in order to construct several classes of meridionally self-similar solutions, and the resulting cases are then summarized in Tables 1 and 2. The general method is next applied in Section 2.2 to a step-by-step construction of a new model for collimated outflows which is also briefly sketched there. In Section 3 the other remaining possibility in spherical coordinates, i.e. radial self-similarity, is taken up. The resulting cases are summarized in Table 3, while a new model is also briefly sketched which gives asymptotically cylindrical, paraboloidal and conical streamlines. Finally, the results are summarized in Section 4.

2 MERIDIONALLY SELF-SIMILAR MHD OUTFLOWS

Consider the steady ($\partial/\partial t = 0$) hydromagnetic equations. They consist of a set of eight coupled, non-linear, partial differential equations expressing momentum, magnetic and mass flux conservation, together with Faraday's law of induction in the ideal MHD limit,

$$\rho(\boldsymbol{V}\cdot\nabla)\boldsymbol{V} = \frac{(\nabla\times\boldsymbol{B})\times\boldsymbol{B}}{4\pi} - \nabla P - \rho\nabla\mathcal{V}\,, \tag{1}$$

$$\nabla\cdot\boldsymbol{B} = 0\,, \quad \nabla\cdot(\rho\boldsymbol{V}) = 0\,, \quad \nabla\times(\boldsymbol{V}\times\boldsymbol{B}) = 0\,. \tag{2}$$

$\boldsymbol{B}$, $\boldsymbol{V}$ and $-\nabla\mathcal{V} = -\nabla(-GM/r)$ denote the magnetic, velocity and external gravity fields, respectively, while ρ and P denote the gas density and pressure. With axisymmetry ($\partial/\partial\phi = 0$), we may introduce the magnetic flux function A, such that three free integrals exist for the total specific angular momentum carried by the flow and the magnetic field, $L(A)$, the corotation angular velocity of each streamline at the base of the flow, $\Omega(A)$, and the ratio of the mass and magnetic fluxes, $\Psi_A(A)$ (Tsinganos 1982). In terms of these integrals and the square of the poloidal Alfvén Mach number (or Alfvén number),

$$M^2 = \frac{4\pi\rho V_{\rm p}^2}{B_{\rm p}^2} = \frac{\Psi_A^2}{4\pi\rho}\,, \tag{3}$$

the magnetic field and bulk flow speed are given in spherical coordinates (r,θ,ϕ) by

$$\boldsymbol{B} = \nabla\times\frac{A(r,\theta)\hat{\boldsymbol{\phi}}}{r\sin\theta} - \frac{L\Psi_A - r^2\sin^2\theta\Omega\Psi_A}{r\sin\theta(1-M^2)}\hat{\boldsymbol{\phi}}\,, \tag{4}$$

$$\boldsymbol{V} = \frac{\Psi_A}{4\pi\rho}\nabla\times\frac{A(r,\theta)\hat{\boldsymbol{\phi}}}{r\sin\theta} + \frac{r^2\sin^2\theta\Omega - LM^2}{r\sin\theta(1-M^2)}\hat{\boldsymbol{\phi}}\,. \tag{5}$$

To construct classes of exact solutions, we shall make two crucial assumptions:

(i) that the Alfvén number M is some function of the dimensionless radial distance $R = r/r_\star$,

$$M = M(R)\,, \tag{6}$$

and

(ii) that the poloidal velocity and magnetic fields have a dipolar angular dependence,

$$A = \frac{r_\star^2 B_\star}{2}\mathcal{A}(\alpha)\,, \qquad \alpha = \frac{R^2}{G^2(R)}\sin^2\theta\,. \tag{7}$$

By choosing $G(R=1) = 1$ at the Alfvén transition $R = 1$, $G(R)$ evidently measures the cylindrical distance ϖ to the polar axis of each fieldline labelled by α, normalized to its cylindrical distance ϖ_α at the Alfvén point, $G(R) = \varpi/\varpi_\alpha$. For a smooth crossing of the Alfvén sphere $R = 1$ [$r = r_\star, \theta = \theta_{\rm a}(\alpha)$], the free integrals L and Ω are related by

$$\frac{L}{\Omega} = \varpi_\alpha^2(A) = r_\star^2\sin^2\theta_{\rm a}(\alpha) = r_\star^2\alpha\,. \tag{8}$$

Therefore the second assumption is equivalent to the statement that at the Alfvén surface the cylindrical distance ϖ_α of each magnetic flux surface $\alpha = $ const and is simply proportional to $\sqrt{\alpha}$.

Note also that the gravitational potential can be expressed in terms of the escape speed $V_{\rm esc}$ at the Alfvén radius $r_\star$,

$$\mathcal{V} = -\frac{\nu^2 V_\star^2}{2R}\,, \qquad \nu = \frac{V_{\rm esc}}{V_\star}\,, \qquad V_{\rm esc} = \sqrt{\frac{2G\mathcal{M}}{r_\star}}\,.$$

Instead of using the three free functions of α, $(\mathcal{A}\,,\Psi_A\,,\Omega)$, we found it more convenient to work instead with the three dimensionless functions of α, $(g_1\,,g_2\,,g_3)$,

$$g_1(\alpha) = \int \mathcal{A}'^2{\rm d}\alpha\,, \tag{9}$$

$$g_2(\alpha) = \frac{r_\star^2}{B_\star^2}\int\Omega^2\Psi_A^2{\rm d}\alpha, \tag{10}$$

$$g_3(\alpha) = \frac{\Psi_A^2}{4\pi\rho_\star}\,. \tag{11}$$

Also, we shall indicate by Π the total pressure in units of the magnetic pressure at the Alfvén surface on the polar axis, $B_\star^2/8\pi = \rho_\star V_\star^2/2$,

$$\Pi = \frac{8\pi}{B_\star^2}\left(P + \frac{B^2}{8\pi}\right),$$

such that

$$P = \frac{B_\star^2}{8\pi}\left(\Pi + f_1 g_1' + f_2\alpha g_1' + f_3\alpha g_2'\right). \tag{12}$$

The functions $f_i(R)$, $i = 1,2,3$, are given in Appendix A, while all starred quantities refer to their respective values at the polar Alfvén

point ($R=1\,,\alpha=0$). Hence

$$\mathcal{A}'(\alpha=0)=1\,,\ \Psi_A(\alpha=0)=\sqrt{4\pi\rho_\star}\,,$$

or

$$g_1'(\alpha=0)=1\,,\ g_3(\alpha=0)=1\,. \tag{13}$$

With assumptions (i)–(ii) and in this notation, the $\hat{\boldsymbol{r}}$- and $\hat{\boldsymbol{\theta}}$-components of the momentum equation become

$$\frac{\partial\Pi(R,\theta)}{\partial R}=f_6g_1'+\left(f_7+\frac{F}{R}f_4\right)\alpha g_1' + \left(f_8+\frac{F}{R}f_5\right)\alpha g_2'+f_9g_3\,, \tag{14}$$

$$\frac{\partial\Pi(R,\theta)}{\partial\theta}=2\cot\theta\left(f_4\alpha g_1'+f_5\alpha g_2'\right). \tag{15}$$

Next, by using α instead of θ as an independent variable, we may transform from the pair of independent variables $(R\,,\theta)$ to the pair of independent variables $(R\,,\alpha)$. With the following elementary relations valid for any differentiable function Φ,

$$\frac{\partial\Phi(R,\theta)}{\partial R}=\frac{\partial\Phi(R,\alpha)}{\partial R}+\alpha\frac{F}{R}\frac{\partial\Phi(R,\alpha)}{\partial\alpha}\,, \tag{16}$$

$$\frac{\partial\Phi(R,\theta)}{\partial\theta}=2\alpha\cot\theta\frac{\partial\Phi(R,\alpha)}{\partial\alpha}\,, \tag{17}$$

we may transform equations (14) and (15) into the following two equations:

$$\frac{\partial\Pi(\alpha,R)}{\partial\alpha}=f_4g_1'+f_5g_2'\,, \tag{18}$$

$$\frac{\partial\Pi(\alpha,R)}{\partial R}=f_6g_1'+f_7\alpha g_1'+f_8\alpha g_2'+f_9g_3\,. \tag{19}$$

By integrating equation (18) we get $\Pi=f_4g_1+f_5g_2+f_0$ where f_0 is an arbitrary function of R. From equation (12) the pressure is

$$P=\frac{B_\star^2}{8\pi}\left(f_4g_1+f_5g_2+f_0+f_1g_1'+f_2\alpha g_1'+f_3\alpha g_2'\right), \tag{20}$$

or,

$$P=\frac{B_\star^2}{8\pi}\mathbf{YP}^\dagger\,,$$

where $\mathbf{P}$ and $\mathbf{Y}$ are the (1×7) matrices

$$\mathbf{P}=\left[\,f_0\ f_4\ f_1\ f_2\ f_5\ f_3\ 0\,\right] \tag{21}$$

and

$$\mathbf{Y}=\left[\,Y_1\ Y_2\ Y_3\ Y_4\ Y_5\ Y_6\ Y_7\,\right]=\left[\,1\ g_1\ g_1'\ \alpha g_1'\ g_2\ \alpha g_2'\ g_3\,\right]. \tag{22}$$

Substituting for Π in equation (19) it follows that

$$-f_9g_3-f_8\alpha g_2'+f_5'g_2-f_7\alpha g_1'-f_6g_1'+f_4'g_1+f_0'=0\,, \tag{23}$$

an expression of the form

$$X_7(R)Y_7(\alpha)+X_6(R)Y_6(\alpha)+\cdots+X_1(R)Y_1(\alpha)=0\,,$$

or,

$$\mathbf{YX}^\dagger=\mathbf{0}\,, \tag{24}$$

with $\mathbf{X}$ the (1×7) matrix:

$$\mathbf{X}=[\,X_1\ X_2\ X_3\ X_4\ X_5\ X_6\ X_7\,] =[\,f_0'\ f_4'\ -f_6\ -f_7\ f_5'\ -f_8\ -f_9\,]\,. \tag{25}$$

2.1 Systematic construction of classes of meridionally self-similar MHD outflows

It is straightforward to prove the following useful theorem (Vlahakis & Tsinganos 1997).

Theorem. If $F_n(\alpha)$, $Y_i(\alpha)$, $X_i(R)$, $i=1,2,\ldots,n$ are arbitrary functions of the independent variables α and R and

$$F_n(\alpha)=Y_1(\alpha)X_1(R)+\cdots+Y_n(\alpha)X_n(R), \tag{26}$$

then there exist constants $c_1,c_2,\ldots,c_n$ such that

$$F_n(\alpha)=c_1Y_1(\alpha)+c_2Y_2(\alpha)+\cdots+c_nY_n(\alpha). \tag{27}$$

Consider then a relation of the form

$$X_n(R)Y_n(\alpha)+\cdots+X_1(R)Y_1(\alpha)=0\,. \tag{28}$$

Regarding the first term of the sum, there are evidently only two possibilities. Either

(i) $X_n(R)=0$ for every R, in which case (indicated by the digit '0') we have

$$X_{n-1}(R)Y_{n-1}(\alpha)+\cdots+X_1(R)Y_1(\alpha)=0\,,$$

or

(ii) $X_n(R)\neq0$, in which case (indicated by the digit '1') we have

$$Y_n(\alpha)=-\frac{X_1(R)}{X_n(R)}Y_1(\alpha)-\cdots-\frac{X_{n-1}(R)}{X_n(R)}Y_{n-1}(\alpha)\,.$$

Then, according to the theorem stated at the beginning of this section, there are constants $\mu_i^{(n)}, i=1,2,\ldots,n-1$, such that $Y_n(\alpha)=\sum_{i=1}^{n-1}\mu_i^{(n)}Y_i(\alpha)$. This gives a condition between the functions of α. Substituting this condition in the initial sum we find

$$\begin{aligned}&[X_{n-1}(R)+\mu_{n-1}^{(n)}X_n(R)]Y_{n-1}(\alpha)\\ &\quad+\left[X_{n-2}(R)+\mu_{n-2}^{(n)}X_n(R)\right]Y_{n-2}(\alpha)\\ &\quad+\ldots+\left[X_1(R)+\mu_1^{(n)}X_n(R)\right]Y_1(\alpha)=0\,.\end{aligned} \tag{29}$$

Hence in both cases (i) and (ii) we find a sum with $n-1$ terms. Following this algorithm, at the end we will have only one term. Since for each product we have the above two possibilities, in total we obtain 2^n cases. Each of them corresponds to a set 'xx...xx' with $x=1,0$ (n digits). The number of '1' digits is the number of conditions between functions of α, while the number of '0' digits is the number of conditions between functions of R.

Following this method, from equation (23) we get 2^7 solutions. Each of them corresponds to a set 'xxxxxxx' with x either 1 or 0. Of those numbers we can say the following.

(i) The first digit is always '1' (because $X_7\neq0$).

(ii) The last digit is always '0' (because $Y_1\neq0$).

(iii)Since $\mathcal{A}'\neq0$, it follows that $g_1'\neq0$ and thus g_1 cannot be a constant. Hence the function $Y_2=g_1$ cannot be proportional to Y_1 and therefore all numbers always have '00' at the end.

(iv) We have in total six unknown functions: the three functions of R, (G,M,f_0) and the three functions of α, (g_1,g_2,g_3). On the other hand, the number of conditions between the functions of R (their number is equal to the number of digits '0') and the functions of α (their number is equal to the number of digits '1') in each one of the sets 'xxxxxxx' is seven. It follows that the system of (G,M,f_0) and $(g_1,\,g_2,\,g_3)$ is overdetermined. Note, however, that since the forms of the functions $X_i(R)$ are more complicated than the forms of the functions $Y_i(\alpha)$, we choose sets 'xxxxxxx' with at most three '0s' because in the case of four or more '0s' we have correspondingly

Table 1. Meridionally self-similar models.

Case	$g_1(\alpha)$	$g_2(\alpha)$	$g_3(\alpha)$	constraints on constants
(1)	α	$\lambda^2\alpha$	$1+\delta\alpha$	
(2)	α	$\xi\alpha+\mu\alpha^\epsilon/\epsilon$	$1+\delta\alpha+\mu\delta_0\alpha^\epsilon$	$\epsilon\neq 0,1, \mu\neq 0$
(3)	α	$\xi\alpha+\mu\alpha\ln\alpha$	$1+\delta\alpha+\mu\delta_0\alpha\ln\alpha$	$\mu\neq 0$
(4)	$\alpha_0 e^{\frac{\alpha}{\alpha_0}}$	$\lambda e^{\frac{\alpha}{\alpha_0}}$	$1+\delta\alpha e^{\frac{\alpha}{\alpha_0}}+\mu\left(e^{\frac{\alpha}{\alpha_0}}-1\right)$	
(5)	$\frac{\alpha_0}{\epsilon}\mid\frac{\alpha}{\alpha_0}-1\mid^{\epsilon-1}\left(\frac{\alpha}{\alpha_0}-1\right)$	$\xi\mid\frac{\alpha}{\alpha_0}-1\mid^\epsilon$	$1+\delta\mid\frac{\alpha}{\alpha_0}-1\mid^\epsilon+\mu\mid\frac{\alpha}{\alpha_0}-1\mid^{\epsilon-1}-\delta-\mu$	$\epsilon\neq 0,1$
(6)	$-\alpha_0\ln\mid\frac{\alpha}{\alpha_0}-1\mid$	$\xi\ln\mid\frac{\alpha}{\alpha_0}-1\mid$	$1+\delta\ln\mid\frac{\alpha}{\alpha_0}-1\mid+\mu\frac{\alpha}{\alpha_0(\alpha-\alpha_0)}$	
(7)	$\frac{\alpha}{1-\alpha_0}$	$\mu\ln\frac{\alpha}{\alpha_0}+\xi\alpha$	$1+\delta(\alpha-\alpha_0)+\mu\delta_0\ln\frac{\alpha}{\alpha_0}$	$\mu\neq 0$
(8)	$\frac{\alpha_0}{\epsilon(1-\alpha_0)}\left(\frac{\alpha}{\alpha_0}\right)^\epsilon$	$\lambda_1\alpha^\epsilon+\lambda_2\alpha^{\epsilon-1}$	$1+\delta_1(\alpha^\epsilon-\alpha_0^\epsilon)+\delta_2(\alpha^{\epsilon-1}-\alpha_0^{\epsilon-1})$	$\epsilon\neq 0,1$
(9)	$\frac{\alpha_0}{1-\alpha_0}\ln\frac{\alpha}{\alpha_0}$	$\lambda_1\ln\frac{\alpha}{\alpha_0}+\frac{\lambda_2}{\alpha}$	$1+\delta_1\ln\frac{\alpha}{\alpha_0}+\delta_2\left(\frac{1}{\alpha}-\frac{1}{\alpha_0}\right)$	

four or more relations between the three functions of R, which in general overdetermines the system of (G, M, f_0). In this way we shift the difficulty of overdetermination of the problem to the set of the three functions of α, (g_1, g_2, g_3), which need to satisfy four relations. In this system, however, it is possible to choose the constants $\mu_i^{(j)}$ such that a consistent solution for the functions of α can be finally constructed.

Altogether, then, and with these considerations in mind, from the $2^7 = 128$ possible cases we end up with only five: 1011100, 1101100, 1110100, 1111000 and 1111100. For each one of those sets we can solve the system for g_1, g_2, g_3, as is shown in the example of the next section.

From a different perspective, $g_1(\alpha)$, $g_2(\alpha)$ and $g_3(\alpha)$ are vectors in a 3D α-space with basis vectors $[u_1(\alpha), u_2(\alpha), u_3(\alpha)]$. This space contains all vectors $g_i(\alpha)$, $i = 1, 2, 3$, subject to the θ-self-similarity constraint manifested by equation (23), i.e. that, for a given such set $g_i(\alpha)$, $i = 1, 2, 3$, the vectors $1, \alpha g_1'(\alpha), \alpha g_2'(\alpha)$ and $g_1'(\alpha)$ also belong to the same space. Each of the resulting functions $g_i(\alpha)$, $i = 1, 2, 3$, is then a linear combination of the basis vectors $u_1(\alpha), u_2(\alpha)$ and $u_3(\alpha)$. In the following, we choose $u_1 = 1$, $u_2 = g_1(\alpha)$. All such sets of basis vectors give all possible meridionally self-similar solutions. Therefore, collecting all possibilities, we end up with the classes of solutions shown in Table 1. Note that in the last three cases $A'(\alpha = 0) \neq 1$, but one can say that the starred quantities refer to values at the point $R = 1, \alpha = \alpha_0 < 1$.

In all nine cases of Table 1, from equations (9), (10) and (11) we may easily find the forms of the free integrals from the relations

$$A = \frac{B_\star r_\star^2}{2}\int_0^\alpha \sqrt{g_1'}\,\mathrm{d}\alpha, \quad \Psi_A = \sqrt{4\pi\rho_\star g_3}\,, \tag{30}$$

$$\Omega = \frac{V_\star}{r_\star}\sqrt{\frac{g_2'}{g_3}}, \quad L = r_\star V_\star \alpha\sqrt{\frac{g_2'}{g_3}}, \tag{31}$$

while, by substituting g_1, g_2 and g_3 in equations (20) and (23), the corresponding *ordinary* differential equations for the jet radius $G(R)$, Alfvén number $M(R)$ and pressure component $f_0(R)$ are found from the R-relations, as is illustrated in the following section.

From the perspective of the α-space, in each one of the cases of Table 1 there exists a 3×7 matrix $\mathbf{K}$ such that

$$\mathbf{Y} = \left[\, u_1 \;\; u_2 \;\; u_3 \,\right]\mathbf{K}, \tag{32}$$

so that, from equation (24),

$$\left[\, u_1 \;\; u_2 \;\; u_3 \,\right]\mathbf{K}\mathbf{X}^\dagger = \mathbf{0}\,.$$

If the u_i are linearly independent then

$$\mathbf{K}\mathbf{X}^\dagger = \mathbf{0}\,.$$

These three equations are the *ordinary* differential equations for the functions of R in each model, while the pressure is

$$P = \frac{B_\star^2}{8\pi}\left[\, u_1 \;\; u_2 \;\; u_3 \,\right]\mathbf{K}\mathbf{P}^\dagger = \frac{B_\star^2}{8\pi}\left(P_0 + P_1 g_1 + P_2 u_3\right),$$

where

$$\mathbf{K}\mathbf{P}^\dagger = [P_0\; P_1\; P_2]^\dagger\,.$$

The first two cases of Table 1 are of some interest. The first is a degenerate one with $u_3 = 0$ and the following form of the free integrals:

$$\begin{aligned} A &= \frac{B_\star r_\star^2}{2}\alpha\,,\ \Psi_A = \sqrt{4\pi\rho_\star(1+\delta\alpha)} \\ \Omega &= \frac{\lambda V_\star}{r_\star}\frac{1}{\sqrt{1+\delta\alpha}}\,. \end{aligned} \tag{33}$$

This is a special case of the more general following case (2) for $\mu = 0$ (and $\xi = \lambda^2$), and has been studied in detail in ST94 and Trussoni et al. (1997). It is the single case where we have only two conditions between the functions of R, so that the third relation between the unknown functions G, M and f_0 is freely chosen. In Trussoni et al. (1997) this corresponds to an a priori specification of the shape of the poloidal streamlines, while in ST94 it corresponds to an a priori imposed relationship between the spherically and non-spherically symmetric components of the pressure. This last case leads to a generalized polytropic-type relation between pressure and density of the form

$$\frac{P(\alpha,R)}{P(0,R)} = \text{ function of } \frac{\rho(\alpha,R)}{\rho(0,R)}\,. \tag{34}$$

As a result, a Bernoulli-type constant exists and, among others, this constant gives a quantitative criterion for the transition of an asymptotically conical wind from an inefficient magnetic rotator to an asymptotically cylindrical jet from an efficient magnetic rotator.

The second case with $\epsilon \neq 0, 1, \mu \neq 0$ has $u_2 = \alpha$, $u_3 = \alpha^\epsilon$. The

Table 2. Meridionally self-similar radial models.

Case	$g_1(\alpha)$	$g_2(\alpha)$	$g_3(\alpha)$
(1)	$-\ln\lvert 1-\alpha\rvert$	0	1
(2)	$\mu\int\frac{\alpha^\epsilon}{1-\alpha}\mathrm{d}\alpha-\ln\lvert 1-\alpha\rvert$	$\lambda^2\frac{\alpha^\epsilon}{\epsilon}$	$1+\delta\alpha^\epsilon$
(3)	$\mu_1\ln\lvert 1-\alpha\rvert+\mu_2\int\frac{\ln\alpha}{1-\alpha}\mathrm{d}\alpha$	$\lambda\ln\alpha$	$\delta_1+\delta_2\ln\alpha$
(4)	$g_1(\alpha)\neq\mu_1\ln\lvert 1-\alpha\rvert+\mu_2$	0	$\delta g_1'(1-\alpha)+\lambda$
(5)	$\mu\ln\lvert 1-\alpha\rvert$	$g_2(\alpha)\neq(\mu,\mu_1\ln\alpha+\mu_2,\mu_1\alpha^{\mu_2}+\mu_3)$	δ

corresponding form of the free integrals is

$$A=\frac{B_\star r_\star^2}{2}\alpha,\ \Psi_A=\sqrt{4\pi\rho_\star\left(1+\delta\alpha+\mu\delta_0\alpha^\epsilon\right)}$$
$$\Omega=\frac{V_\star}{r_\star}\sqrt{\frac{\mu\alpha^{\epsilon-1}+\xi}{1+\delta\alpha+\mu\delta_0\alpha^\epsilon}}. \tag{35}$$

This is a new case which emerged from the present systematic construction. The corresponding differential equations are derived in detail in the example of the next section where the solution is briefly analysed.

In the special configuration with $G=R\Leftrightarrow\alpha=\sin^2\theta$, the field- and streamlines on the poloidal plane are radial and we find the five cases shown in Table 2.

The first case is a *degenerate* one, wherein there is only one condition between the unknown functions $M(R)$ and $f_0(R)$. Thus a second relation between $M(R)$ and $f_0(R)$ can be imposed a priori, for example a polytropic relation between pressure and density. This last possibility leads precisely to Parker's (1958) classical solar wind solution with a radial and non-rotating outflow. All other cases (2)–(5) are *non-degenerate*, i.e. there are two relations between $M(R)$ and $f_0(R)$.

The second case has been analysed in detail in Lima et al. (1996) and corresponds to a radial but heliolatitudinally dependent outflow. If in addition $\mu=-1,\epsilon=1$, this case coincides with (1) in Table 1 for radial poloidal streamlines. Note that a common feature of all rotating cases with radial streamlines on the poloidal plane is that they cannot be extended over all of the poloidal plane, for sufficiently fast magnetic rotators. For example, in the model of Lima et al.. (1996) the pressure becomes negative at some colatitude $\theta_{\max}$, for large values of rotation. This is basically due to the fact that, with the poloidal magnetic field dropping like $1/R^2$ and the azimuthal field dropping like $1/R$, the magnetic pressure drops like $1/R^4$ and by itself alone cannot balance the magnetic tension which drops like $1/R^3$; a strong pressure gradient is then needed from the pole towards the equator to balance the magnetic pinching. In fast magnetic rotators this pressure gradient is so strong that it leads to negative values of the pressure at angles $\theta>\theta_{\max}$. A collimated outflow with uniform asymptotic conditions is the only way left for an everywhere valid outflow from an efficient magnetic rotator (Heyvaerts & Norman 1989; ST94).

2.2 Example of a new model for a meridionally self-similar MHD outflow

Let us illustrate the previous construction with the example 1101100 obtained from the present case with $n=7$. This number has the following meaning.

Since the first digit is 1, there are six constants $\mu_i^{(7)}, i=1,2,\ldots,6$ such that the following relation holds between the functions $Y_i(\alpha), i=1,2,\ldots 7$:

$$Y_7=\sum_{i=1}^{6}\mu_i^{(7)}Y_i\qquad(\alpha\text{-relation-1})\,. \tag{36}$$

Substituting this expression for Y_7 in the initial relation equation (24) between the functions $(X_i, Y_i), i=1,\ldots,7$, we obtain

$$\left(X_6+\mu_6^{(7)}X_7\right)Y_6+\left(X_5+\mu_5^{(7)}X_7\right)Y_5 +\ldots+\left(X_1+\mu_1^{(7)}X_7\right)Y_1=0\,. \tag{37}$$

Now the second digit is again 1 and thus there are five constants $\mu_i^{(6)}, i=1,2,\ldots,5$ such that

$$Y_6=\sum_{i=1}^{5}\mu_i^{(6)}Y_i\qquad(\alpha\text{-relation-2})\,, \tag{38}$$

while substituting this relation in equation (39) we obtain

$$\left[\left(X_5+\mu_5^{(7)}X_7\right)+\mu_5^{(6)}\left(X_6+\mu_6^{(7)}X_7\right)\right]Y_5 +\ldots+\left[\left(X_1+\mu_5^{(7)}X_7\right)+\mu_1^{(6)}\left(X_6+\mu_6^{(7)}X_7\right)\right]Y_1=0\,. \tag{39}$$

The third digit is 0 and hence

$$\left(X_5+\mu_5^{(7)}X_7\right)+\mu_5^{(6)}\left(X_6+\mu_6^{(7)}X_7\right)=0\qquad(R\text{-relation-1}), \tag{40}$$

a relation between the functions of R. With the help of equation (42), equation (41) now reduces to

$$\sum_{i=1}^{4}\left[\left(X_i+\mu_i^{(7)}X_7\right)+\mu_i^{(6)}\left(X_6+\mu_6^{(7)}X_7\right)\right]Y_i=0\,. \tag{41}$$

The fourth digit is 1 and thus there are three constants $\mu_i^{(4)}, i=1,2,3$, such that

$$Y_4=\sum_{i=1}^{3}\mu_i^{(4)}Y_i\qquad(\alpha\text{-relation-3})\,. \tag{42}$$

Substituting this relation in equation (43) we obtain

$$\sum_{i=1}^{3}\{[(X_i+\mu_i^{(7)}X_7)+\mu_i^{(6)}(X_6+\mu_6^{(7)}X_7)] +\mu_i^{(4)}[(X_4+\mu_4^{(7)}X_7)+\mu_4^{(6)}(X_6+\mu_6^{(7)}X_7)]\}Y_i=0\,. \tag{43}$$

The fifth digit is 1 and there are two constants $\mu_i^{(3)}, i=1,2$, such that

$$Y_3=\mu_1^{(3)}Y_1+\mu_2^{(3)}Y_2\qquad(\alpha\text{-relation-4})\,. \tag{44}$$

Substituting this in equation (43) we find a relation involving Y_1 and Y_2. Finally, we must put equal to zero the multipliers of Y_1, Y_2 in this

relation because the two remaining digits are 0. So we have

$$\begin{aligned}&\left[\left(X_i+\mu_i^{(7)}X_7\right)+\mu_i^{(6)}\left(X_6+\mu_6^{(7)}X_7\right)\right]\\&\quad+\mu_i^{(4)}\left[\left(X_4+\mu_4^{(7)}X_7\right)+\mu_4^{(6)}\left(X_6+\mu_6^{(7)}X_7\right)\right]\\&\quad+\mu_i^{(3)}\left\{\left[\left(X_3+\mu_3^{(7)}X_7\right)+\mu_3^{(6)}\left(X_6+\mu_6^{(7)}X_7\right)\right]\right.\\&\quad\left.+\mu_3^{(4)}\left[\left(X_4+\mu_4^{(7)}X_7\right)+\mu_4^{(6)}\left(X_6+\mu_6^{(7)}X_7\right)\right]\right\}=0\,,\end{aligned}\tag{45}$$

for $i=1,2$ (R-relations-2,3) .

These last two equations together with equation (40) are the three equations for the functions of R. On the other hand, equations (36), (38), (42) and (44) are four relations among the three functions of α. These relations of the functions of α [equations (44), (42), (38) and (36)] are equivalent to the system

$$\left.\begin{array}{l}Y_3=c_1Y_1+c_2Y_2\\Y_4=c_3Y_1+c_4Y_2\\Y_6=c_5Y_1+c_6Y_2+c_7Y_5\\Y_7=c_8Y_1+c_9Y_2+c_{10}Y_5\end{array}\right\}\Leftrightarrow\left\{\begin{array}{l}g_1'=c_1+c_2g_1\\\alpha g_1'=c_3+c_4g_1\\\alpha g_2'=c_5+c_6g_1+c_7g_2\\g_3=c_8+c_9g_1+c_{10}g_2.\end{array}\right.$$

Note that we have renamed the constants and also used equation (22). From the first, if $c_2\neq0$ it follows that $g_1=-c_1/c_2+ce^{c_2\alpha}$. Then, from the second $c=0$ and hence $g_1=-c_1/c_2$. However, g_1 cannot be a constant. Thus, $c_2=0$, and the first two equations combined with equation (13) give $g_1=\alpha+c_{11}$, while the third has the solutions

$$g_2=\begin{cases}\dfrac{c_6}{1-c_7}\alpha+c_{12}+c_{13}\alpha^{c_7}, & \text{if } c_7\neq0,1,\\ c_6\alpha\ln\alpha+c_{14}+c_{15}\alpha\,, & \text{if } c_7=1,\\ c_6\alpha+c_{16}\ln\alpha+c_{17}\,, & \text{if } c_7=0.\end{cases}$$

For the first possibility, we have finally the second case of Table 1:

$$g_1=\alpha,$$

$$g_2=\xi\alpha+\frac{\mu\alpha^{\epsilon}}{\epsilon}\,,\qquad\epsilon\neq0,1,$$

$$g_3=1+\delta\alpha+\mu\delta_0\alpha^{\epsilon},$$

where we have absorbed the constants c_{11},c_{12} in the unknown function f_0, $c_{11}f_4+c_{12}f_5+f_0\rightarrow f_0$, equations (20), (23).

After substituting these values of g_1,g_2 and g_3 in equations (20)–(23), we find that

$$\begin{aligned}&\left[f_0'-f_6-f_9\right]+\left[f_4'+\xi f_5'-f_7-\xi f_8-\delta f_9\right]\alpha\\&\quad+\mu\left[f_5'/\epsilon-f_8-\delta_0f_9\right]\alpha^{\epsilon}=0\,,\end{aligned}\tag{46}$$

and

$$\begin{aligned}P&=\frac{B_\star^2}{8\pi}\left(P_0+P_1\alpha+P_2\alpha^{\epsilon}\right)\\&=\frac{B_\star^2}{8\pi}\left[f_0+f_1+\left(f_4+\xi f_5+f_2+\xi f_3\right)\alpha+\mu\left(\frac{f_5}{\epsilon}+f_3\right)\alpha^{\epsilon}\right].\end{aligned}\tag{47}$$

By setting equal to zero the three expressions in the square brackets of equation (46) (since $\mu\neq0$ and $1\,,\alpha$ and α^{ϵ} are linearly independent vectors in the α-space for $\epsilon\neq0,1$) we find the three R-relations for the functions $G(R),M(R)$ and $f_0(R)$ [which are the same with equations (42) and (45)]. Using the functions f_4 and F and the definitions of P_0 and P_1 we obtain five, *first order*, ordinary differential equations for $G(R)$, $F(R)$, $M(R)$ and the two pressure components $P_1(R)$ and $P_0(R)$,

$$\frac{\mathrm{d}G^2}{\mathrm{d}R}=-\frac{F-2}{R}G^2,\tag{48}$$

$$\begin{aligned}\frac{\mathrm{d}F}{\mathrm{d}R}&=\frac{F}{1-M^2}\frac{\mathrm{d}M^2}{\mathrm{d}R}-\frac{F(F-2)}{2R}\\&\quad-\frac{F^2-4}{2R(1-M^2)}-\frac{2G^2RP_1}{1-M^2}\\&\quad-\frac{2\xi R}{M^2(1-M^2)^3}[(2M^2-1)G^4-M^4+2M^2(1-G^2)],\end{aligned}\tag{49}$$

$$\begin{aligned}\frac{\mathrm{d}M^2}{\mathrm{d}R}&=\frac{M^2(1-M^2)}{(2M^2-1)G^4-M^4}\left\{-\epsilon\delta_0\nu^2\frac{G^2(1-M^2)}{R^2}\right.\\&\quad\left.+\frac{F-2}{R}[(\epsilon+1)M^2-(\epsilon-1)G^4]\right\},\end{aligned}\tag{50}$$

$$\begin{aligned}\frac{\mathrm{d}P_1}{\mathrm{d}R}&=-\left[\frac{F^2-4}{2R^2G^2}+2\xi\frac{(1-G^2)}{G^2(1-M^2)^3}\right]\frac{\mathrm{d}M^2}{\mathrm{d}R}\\&\quad-\frac{M^2F}{2R^2G^2}\frac{\mathrm{d}F}{\mathrm{d}R}-\frac{\delta\nu^2}{R^2M^2}-\frac{M^2(F^2-4)(F-4)}{4R^3G^2}\\&\quad+\xi\frac{(F-2)[(2M^2-1)G^4-M^4]}{RG^2M^2(1-M^2)^2},\end{aligned}\tag{51}$$

$$\frac{\mathrm{d}P_0}{\mathrm{d}R}=-\frac{2}{G^4}\frac{\mathrm{d}M^2}{\mathrm{d}R}-\frac{\nu^2}{R^2M^2}-\frac{2M^2(F-2)}{RG^4}.\tag{52}$$

Note that the third pressure component $P_2(R)$ is given explicitly in terms of M and G (f_3 and f_5). An integration of the above set of equations will give the complete solution. However, this exercise is rather complicated since any physically accepted solution should pass through the various MHD critical points (Tsinganos et al. 1996). This undertaking, together with a discussion of the solution and application to collimated outflows, is the subject of our next paper.

It is worth mentioning at this point that our analysis of model (2) of Table 1 shows that mainly cylindrically collimated solutions are obtained. The set of Figs 1 and 2 illustrates such a typical solution for a representative set of the constants describing the particular model. This solution crosses the Alfvén surface for appropriate values of the slope of the square of the Alfvén number $p_\star=\left(\mathrm{d}M^2/\mathrm{d}R\right)_\star$, the expansion function $F_\star$ and $P_{1\star}$ which satisfy the Alfvén regularity condition (Heyvaerts & Norman 1989; ST94) which is easily obtained from equation (77) of Appendix A at $(R=G=M=1)$, i.e.

$$F_\star p_\star=2f_{4\star}\,.\tag{53}$$

The non-spherically symmetric part of the pressure $P_{1\star}$ is obtained from its definition while the functions $f_{3\star}$ and $f_{5\star}$ are calculated for $R=1$ using the L'Hospital rule. Figs 1–3 correspond to the set $F_\star=1.1$ and $p_\star=1.6$. Note that after the Alfvén star-type critical point is crossed, the (modified by self-similarity) X-type fast critical point (Tsinganos et al. 1996) may be crossed by further adjusting appropriately the triplet of the variables $(F_\star\,,p_\star\,,P_{1\star})$. It suffices to note that solutions crossing only the Alfvén surface do not differ qualitatively from those that in addition cross the (modified by the present meridional self-similarity) fast critical surface.

Fig. 1 shows the shape of the streamlines on the poloidal plane and close to the Alfvén surface. The cylindrical asymptotic shape of the poloidal streamlines may be better seen in the enlarged scale of Fig. 2. Note also the constant wavelength but the amplitude of oscillation decaying with distance, in full agreement with the analysis in Vlahakis & Tsinganos (1997). At the last displayed

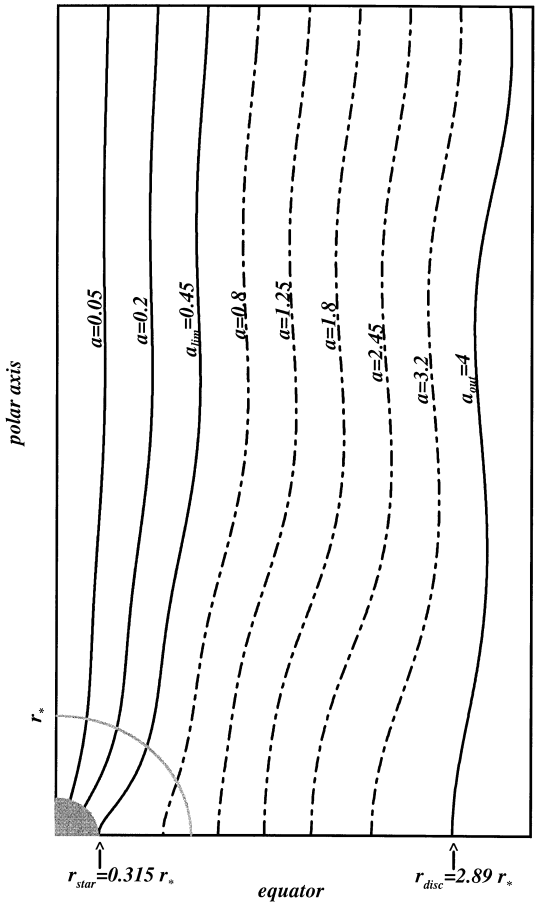

Figure 1. Poloidal field and streamlines close to the stellar base for the asymptotically cylindrical θ-self-similar model of case (2) from Table 1, for the following set of parameters: $\epsilon = 0.5$, $\nu^2 = 2\mathcal{G}M/r_\star V_\star^2 = 10$, $\delta\nu^2 = 3.5$, $\delta_0\nu^2 = 0.1$, $\xi = -10$, $\mu = 20$, $p_\star = \left(\mathrm{d}M^2/\mathrm{d}R\right)_\star = 1.6$, $F_\star = 1.1$.

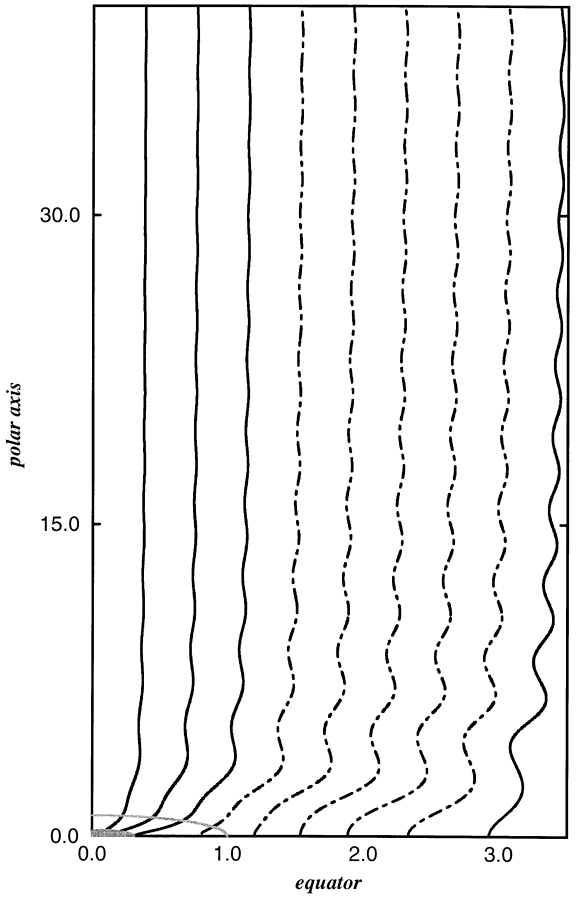

Figure 2. Poloidal field and streamlines as in Fig. 1, but on an enlarged scale to show the asymptotic collimation reached after the oscillations have decayed.

fieldline $\alpha_{\rm out} = 4$, the toroidal fields vanish, $B_\phi = 0$, $V_\phi = 0$. For $\alpha > \alpha_{\rm out}$, Ω^2 becomes negative, so there is no solution there. The same oscillatory behaviour can be seen in the fieldlines that are not attached to the star but are perpendicular to a thin disc around it (dash-dotted curves in Figs 1 and 2). The oscillatory structure of all flow speeds before the flow reaches full cylindrical collimation is also shown in Fig. 3 where we have plotted the characteristic velocities in units of the Alfvén speed at the polar axis and the Alfvén sphere ($\alpha = 0, R = 1$), $V_\star$.

The poloidal speed along the polar axis $V_{\rm p,pol}$ increases to a uniform superAlfvénic value and is higher than the same speed along the limiting streamline $V_{\rm p,lim}$ (i.e. the last fieldline attached to the stellar base $r_{\rm star}$ taken to be at $0.315r_\star$). Both reach asymptotically uniform values after $V_{\rm p,lim}$ intersects the curve of the poloidal Alfvén speed $V_{\rm Ap,lim}$ at $R = 1$. Note that corotation may be seen up to the Alfvén distance $R = 1$: the azimuthal speed $V_{\phi,\rm lim}$ at the 'limiting fieldine' increases until the Alfvén surface is reached and drops from angular momentum conservation as the outflow expands almost conically. Further away, however, this speed too levels off to a constant value when full collimation is achieved, as expected. Finally, the fact that the jet has a large component of toroidal field is reflected by the large values of the Alfvén speed associatd with the toroidal magnetic field, $V_{\rm A\phi,lim}$, as compared with the rotational speed $V_{\phi,\rm lim}$.

3 SYSTEMATIC CONSTRUCTION OF CLASSES OF RADIALLY SELF-SIMILAR MHD OUTFLOWS

To construct general classes of radially self-similar solutions, we make the following two key assumptions: (i) the Alfvén Mach number M is solely a function of θ,

$$M = M(\theta)\,, \qquad M(\theta_\star) = 1\,, \tag{54}$$

and (ii) the poloidal velocity and magnetic fields have a dipolar angular dependence,

$$A = \frac{B_0\varpi_0^2}{2}\mathcal{A}(\alpha)\,, \qquad \alpha = \frac{R^2}{G^2(\theta)}\sin^2\theta\,, \quad R = \frac{r}{\varpi_0}\,, \tag{55}$$

where B_0 and ϖ_0 are constants. By choosing $G\left(\theta_\star\right) = 1$ at the Alfvén transition $\theta_\star$, $G(\theta)$ evidently measures the cylindrical distance ϖ to the polar axis of each fieldline labelled by α, normalized to its cylindrical distance ϖ_α at the Alfvén point, $G(\theta) = \varpi/\varpi_\alpha$. For a smooth crossing of the Alfvén cone $\theta = \theta_\star$ [$r = r_\alpha(\alpha), \theta = \theta_\star$], the free integrals L and Ω are related by

$$\frac{L}{\Omega} = \varpi_\alpha^2(A) = r_\alpha^2(\alpha)\sin^2\theta_\star = \varpi_0^2\alpha\,. \tag{56}$$

Therefore the second assumption is equivalent to the statement that, at the Alfvén conical surface, the cylindrical distance $\varpi_{\rm a}$ of each magnetic flux surface $\alpha = $ const and is simply proportional to $\sqrt{\alpha}$, exactly as in the previous meridionally self-similar case.

Instead of using the three functions of α, ($\mathcal{A}$, Ψ_A, Ω), we found it

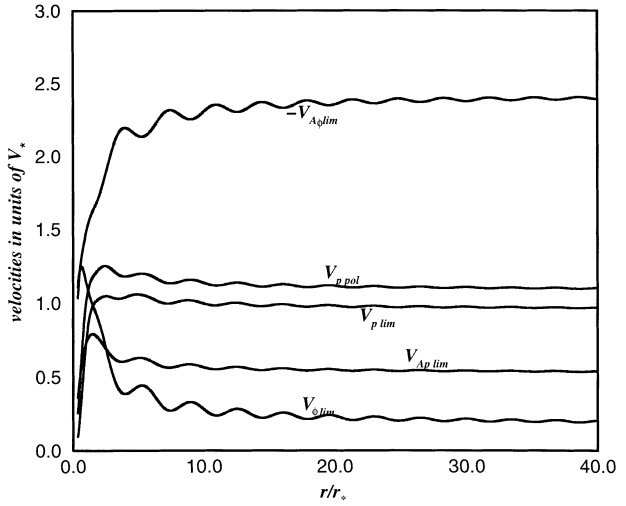

Figure 3. Outflow velocities in units of $V_\star$, the radial speed at the Alfvén point ($\alpha = 0, R = 1$), for the parameters given in the caption of Fig. 1 of model (2) of Table 1.

more convenient to work with the three dimensionless functions of α, $(q_1\,, q_2\,, q_3)$,

$$q_1(\alpha) = \int \frac{\mathcal{A}^{'2}}{\alpha}\mathrm{d}\alpha\,, \tag{57}$$

$$q_2(\alpha) = \frac{\varpi_0^2}{B_0^2}\int \Omega^2 \Psi_A^2 d\alpha\,, \tag{58}$$

$$q_3(\alpha) = \frac{\mathcal{G}M}{B_0^2\varpi_0}\int \frac{\Psi_A^2}{\alpha^{\frac{3}{2}}}\mathrm{d}\alpha\,. \tag{59}$$

Following the same algorithm as in the previous case, we shall use $(\alpha\,, \theta)$ as the independent variables and transform the derivatives with respect to $\boldsymbol{r}$ and $\boldsymbol{\theta}$ to derivatives with respect to α and θ in the $\hat{\boldsymbol{r}}$- and $\hat{\boldsymbol{\theta}}$-components of the momentum equation. Integrating the resulting $\hat{\boldsymbol{r}}$-component of the momentum equation, we get

$$P = \frac{B_0^2}{8\pi}\left(h_1\alpha q_1' + h_2\alpha q_2' + h_3 q_2 + h_4 q_3 + h_5 q_1 + h_0\right), \tag{60}$$

or

$$P = \frac{B_o^2}{8\pi}\mathbf{Y}\mathbf{P}^\dagger$$

with

$$\mathbf{P} = \left[\, h_0\; h_5\; h_1\; h_3\; h_2\; h_4\; 0\,\right], \tag{61}$$

and

$$\mathbf{Y} = \left[\, Y_1\; Y_2\; Y_3\; Y_4\; Y_5\; Y_6\; Y_7\,\right]$$
$$= \left[\, 1\; q_1\; \alpha q_1'\; q_2\; \alpha q_2'\; q_3\; \alpha q_3'\,\right], \tag{62}$$

and after substituting the pressure in the other component of the momentum equation we obtain

$$Hh_4\alpha q_3' + h_4' q_3 + h_3(H-2)\alpha q_2' + h_3' q_2 + \frac{\left[h_1\left(1-M^2\right)^2\right]'\alpha q_1'}{\left(1-M^2\right)} + h_5' q_1 + h_0' = 0 \tag{63}$$

where a prime in the functions of $q_i(\alpha)$, $i = 1, 2, 3$, and h_i indicates a derivative with respect to their variables α and $\ln\sin\theta$, respectively, while the functions $h_j(\theta), j = 1, 2, 3, 4, 5$, and H are given in Appendix B.

This expression is again of the form

$$X_7(\theta)Y_7(\alpha) + X_6(\theta)Y_6(\alpha) + \cdots + X_1(\theta)Y_1(\alpha) = 0, \text{ or } \mathbf{X}\mathbf{Y}^\dagger = \mathbf{0}, \tag{64}$$

with $\mathbf{X}$ the (1×7) matrix

$$\mathbf{X} = \left[\, X_1\; X_2\; X_3\; X_4\; X_5\; X_6\; X_7\,\right]$$
$$= \left[\, h_0'\; h_5'\; \frac{\left[h_1\left(1-M^2\right)^2\right]'}{\left(1-M^2\right)}\; h_3'\; h_3(H-2)\; h_4'\; Hh_4\,\right]. \tag{65}$$

As in the previous case of meridionally self-similar solutions, we classify the various possibilities by the sets 'xxxxxxx'. These sets always have '00' at the end, their first digit is '1' and they have at most three '0s', while from the 2^7 possibilities we end up again with the cases 1011100, 1101100, 1110100, 1111000 and 1111100. Now the vectors $q_1(\alpha)$, $q_2(\alpha)$ and $q_3(\alpha)$ belong to a 3D α-space with basis vectors $[e_1(\alpha)\,, e_2(\alpha)\,, e_3(\alpha)]$. This space contains all vectors $q_i(\alpha)$, $i = 1, 2, 3$, subject to the r-self-similarity constraint manifested by equation (63), i.e. that for a given such set $q_i(\alpha)$, $i = 1, 2, 3$, the vectors $1, \alpha q_i'(\alpha)$, $i = 1, 2, 3$, also belong to the same space. Each of the functions $q_i(\alpha)$, $i = 1, 2, 3$, that satisfies this constraint is then a linear combination of the basis vectors $e_1(\alpha)$, $e_2(\alpha)$ and $e_3(\alpha)$. In the following, we choose $e_1 = 1$, $e_2 = q_1(\alpha)$. All such sets of basis vectors give all possible radially self-similar solutions. Therefore, collecting all possibilities, we end up with the six classes of solutions shown in Table 3.

In all of the cases of Table 3, from equations (57), (58) and (59) we find the form of the functions of α,

$$A = \frac{B_0\varpi_0^2}{2}\int_0^\alpha \sqrt{\alpha q_1'}\mathrm{d}\alpha\,, \quad \Psi_A^2 = \frac{B_0^2\varpi_0}{\mathcal{G}\mathcal{M}}\alpha^{\frac{3}{2}}q_3',$$

$$\Omega^2 = \frac{\mathcal{G}\mathcal{M}}{\varpi_0^3}\frac{q_2'}{q_3'}\alpha^{-\frac{3}{2}}, \quad L^2 = \mathcal{G}\mathcal{M}\varpi_0\frac{q_2'}{q_3'}\alpha^{\frac{1}{2}}. \tag{66}$$

Table 3. Radially self-similar models.

Case	$q_1(\alpha)$	$q_2(\alpha)$	$q_3(\alpha)$	constants
(1)	$\frac{E_1}{F-2}\alpha^{F-2}$	$\frac{D_1}{F-2}\alpha^{F-2}$	$\frac{C_1}{F-2}\alpha^{F-2}$	$E_1, F-2\neq 0$
(2)	$E_1\ln\alpha$	$D_1\ln\alpha$	$C_1\ln\alpha$	$E_1\neq 0$
(3)	$E_1\alpha^{x_1}+E_2\alpha^{x_2}$	$D_1\alpha^{x_1}+D_2\alpha^{x_2}$	$C_1\alpha^{x_1}+C_2\alpha^{x_2}$	$E_1^2+D_1^2+C_1^2, E_2, x_1, x_2, x_1-x_2\neq 0$
(4)	$E_1\ln\alpha+E_2\alpha^x$	$D_1\ln\alpha+D_2\alpha^x$	$C_1\ln\alpha+C_2\alpha^x$	$E_i^2+D_i^2+C_i^2, x\neq 0, i=1,2$
(5)	$E_1(\ln\alpha)^2+E_2\ln\alpha$	$D_1(\ln\alpha)^2+D_2\ln\alpha$	$C_1(\ln\alpha)^2+C_2\ln\alpha$	$E_1^2+D_1^2+C_1^2\neq 0$
(6)	$E_1\alpha^x\ln\alpha+E_2\alpha^x$	$D_1\alpha^x\ln\alpha+D_2\alpha^x$	$C_1\alpha^x\ln\alpha+C_2\alpha^x$	$E_1^2+D_1^2+C_1^2\neq 0$

Finally, by substituting q_1, q_2 and q_3 in equations (60) and (63), we find the ordinary differential equations which the functions $G(\theta)$, $M(\theta)$ and $h_0(\theta)$ obey.

In α-space, for each of the cases of Table 3 there exists a (3×7) matrix $\mathbf{K}$ such that

$$\mathbf{Y} = \left[\, e_1 \;\; e_2 \;\; e_3 \,\right] \;\mathbf{K}, \tag{67}$$

and from equation (64)

$$\left[\, e_1 \;\; e_2 \;\; e_3 \,\right] \mathbf{K}\mathbf{X}^{\dagger} = \mathbf{0}.$$

If the basis vectors e_i are linearly independent, then

$$\mathbf{K}\mathbf{X}^{\dagger} = \mathbf{0}.$$

These three equations are the *ordinary* differential equations for the functions of θ in each model of Table 3, while for the pressure

$$P = \frac{B_o^2}{8\pi}\left[\, e_1 \;\; e_2 \;\; e_3 \,\right]\mathbf{K}\mathbf{P}^{\dagger} = \frac{B_\star^2}{8\pi}\left(P_0 + P_1 q_1 + P_2 e_3\right),$$

where

$$\mathbf{K}\mathbf{P}^{\dagger} = \left[P_0 \; P_1 \; P_2\right]^{\dagger}.$$

As with the previous meridionally self-similar solutions, the first two classes are of particular interest. The first corresponds to the following form of the free integrals:

$$A = \frac{B_0 \varpi_0^2 \sqrt{E_1}}{F}\alpha^{\frac{F}{2}},\;\; \Psi_A^2 = \frac{C_1 B_0^2 \varpi_0}{\mathcal{G}M}\alpha^{(F-3/2)},\; \Omega^2 = \frac{D_1 \mathcal{G}M}{\varpi_0^3 C_1}\alpha^{-\frac{3}{2}}. \tag{68}$$

This is a degenerate case, i.e. $e_3 = 0$ and we have only two conditions between the functions of θ. It follows that we are free to impose a third relation between the unknown functions $[G(\theta), M(\theta), h_0(\theta)]$. One possibility is that such a third imposed relation is of the polytropic type, $P \propto \rho^{\gamma}$ (in this case $h_0 = 0$). In such a polytropic case, which has been analysed in detail by Contopoulos & Lovelace (1994), the magnetic flux is of the form $A = f_f(\theta)R^F$ with $f_f(\theta) \propto [\sin\theta/G(\theta)]^F$ (for notation see also Tsinganos et al. 1996). The magnetic field at the equatorial plane $\theta = 90°$ is $B \propto R^{F-2}$, the density $\rho \propto R^{2F-3}$, while the sound, Alfvén and rotational speeds scale as their Keplerian counterparts, i.e. as $R^{-1/2}$. Note that if $[D_1 G(\pi/2)/C_1]\left[(G^2 - M^2)/G\left(1 - M^2\right)\right]^2_{\theta=\frac{\pi}{2}} = 1$, the rotational velocity at the equatorial plane is exactly Keplerian. The classical and simplest subcase analysed in BP82 corresponds to the subclass with $F = 3/4$, wherein $B \propto R^{-5/4}$. The two relations among the functions of θ are the two resulting first-order differential equations for the Alfvén number $M(\theta)$ and dimensionless radius $G(\theta)$ [$m(\chi) = M^2(\theta)$ and $\xi(\chi) = G(\theta)/G(\frac{\pi}{2})$ in the notation of BP82].

The second case is also degenerate since $e_3 = 0$ with again only two conditions between the functions of θ. As before, we are free to impose a third relation between the unknown functions $[G(\theta), M(\theta), h_0(\theta)]$: for example, a polytropic relationship. Then one can prove that this case is a subcase of the first one (if it is polytropic), for $F = 2$. All other cases shown in Table 3 are non-degenerate.

The third class is characterized *first* by a set of parameters describing the particular model and the dependence of the free integrals on the magnetic flux function $A(\alpha)$, $(x_1, x_2, E_1, E_2, C_1, C_2, D_1, D_2)$, *secondly* by the Alfvén angle $\theta_\star$, and *thirdly*, by the set of critical point parameters $p_\star = \left(\mathrm{d}M^2/\mathrm{d}\theta\right)_\star$ and $\varphi_\star$ which denote the slope of the Alfvén number and the expansion angle, respectively, at the Alfvén angle $\theta_\star$, together with the pressure component $P_{1\star}$ through $h_{5\star}$. This triplet of 'dynamical' parameters fixes the physical solution, and they are related through the Alfvén regularity condition which is now obtained from

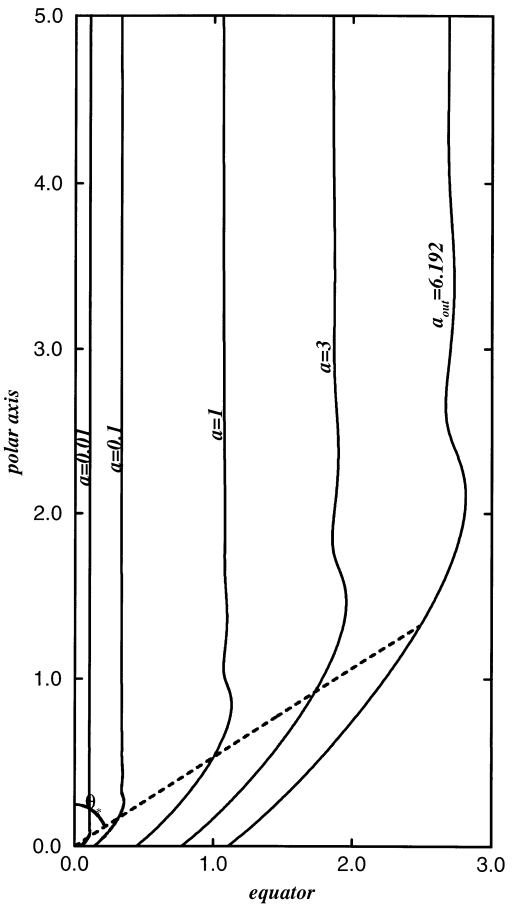

Figure 4. Field and streamlines for the cylindrical r-self-similar model of case (3) from Table 3 and the following set of parameters: $x_1 = -0.6$, $x_2 = -0.5$, $E_1 = -0.03$, $E_2 = 0.03$, $C_1 = -1.5$, $C_2 = -0.6$, $D_1 = -25$, $D_2 = -10$, $\theta_\star = 62°$, $\varphi_\star = 55°$, $p_\star = -3$. At the disc level, $V_\phi \propto R^{-1/2}$, while on the poloidal field/streamline $\alpha_{\rm out} = 6.191\,736$, $B_{\rm p} = V_{\rm p} = 0$.

equation (92) of Appendix B at the Alfvén angle $\theta_\star$ where $M = G = 1$ and $h_5 = h_{5\star}$, i.e.

$$h_{5\star} = -\sin^2\theta_\star \tan(\theta_\star + \varphi_\star) p_\star. \tag{69}$$

As with the previous case of meridional self-similarity, this condition relates the slope of the square of the Alfvén number $p_\star = \left(\mathrm{d}M^2/\mathrm{d}\theta\right)_\star$ and the expansion angle $\varphi_\star$ with the pressure component $P_{1\star}$ through $h_{5\star}$. Finally, the requirement that the solution crosses the two slow and fast X-type critical points [modified by the radial self-similarity assumption (Tsinganos et al. 1996)] determines all these three 'dynamical' parameters $[\varphi_\star, p_\star, P_{1\star}]$.

It is interesting to note that, contrary to classes (1)–(2) in Table 3, this model (3) may be characterized by a scale, for example the radial distance on the plane of the disc where the magnitudes of the poloidal speed and magnetic field or the toroidal speed and magnetic field become zero. Hence it occurred to us that this is an interesting generalization of the BP82 model and therefore worthy of further investigation.

Figs 4 and 5 are a typical illustration of model (3) for describing collimated jet-type outflows *with* an oscillatory behaviour. In Fig. 4 the poloidal field and streamlines reach a cylindrical shape after undergoing oscillations in their radius. As we move downstream, the amplitude of these oscillations decays while their wavelength increases. In fact, the exact behaviour of the oscillations is

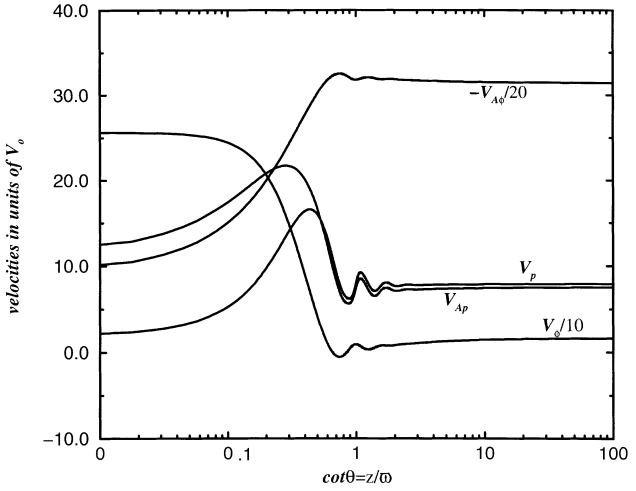

Figure 5. The characteristic velocities of model (3) of Table 3 with cylindrical asymptotics are plotted in units of the z-component of the flow speed at the point $(\alpha = 1, \theta = \pi/2)$, V_0 and for the same parameters as in Fig. 4.

analytically described by Vlahakis & Tsinganos (1997), where it is shown that they can be regarded as perturbations on an asymptotically cylindrical shape which can be expressed in terms of the Legendre functions $P_\nu^\mu(\cos\theta)$ and $Q_\nu^\mu(\cos\theta)$. According to this analysis, when $\mu^2 < 0$, the asymptotically cylindrical shape is finally obtained through those oscillations. Then the perturbation (for $\theta \to 0$) is proportional to $\theta^{\pm\mu-\nu}$, or, since $\mu^2 < 0$, proportional to $\left(\frac{\varpi}{z}\right)^{-\nu} \cos\left(|\mu| \ln\frac{\varpi}{z} + D_0\right)$. In the example shown in Figs 4 and 5 the amplitude of the oscillations is rather weak. Note, however, that cases also exist with an extremely strong oscillation amplitude, and such examples will be analysed in another connection. On the other hand, when $\mu^2 \geq 0$ the asymptotically cylindrical shape is reached without such oscillations. Exactly this last possibility is shown in the following case of (Figs 6 and 7).

To illustrate further the various possibilities for the asymptotic behaviour of outflows starting from a Keplerian disc, we examine briefly the group of three models in Figs 6–7, 8–9 and 10–11 where, depending on the values of the model constants, we obtain one with cylindrical, parabolical or conical terminal geometry.

(1) In Figs 6 and 7 a *cylindrically* collimated outflow [when $\theta \to 0, (M^2, G^2) \to$ constants] is obtained for a set of model parameters $(x_i, E_i, C_i, D_i), i = 1, 2$. The Alfvén conical surface is taken at $\theta_\star = 60°$ where the slope of the square of the Alfvén number is fixed as $p_\star = -1.1$, while the expansion angle $\varphi_\star \approx 75°$ (the angle of the poloidal streamline with the cylindrical radius). The characteristic scale of the model is taken to indicate approximately the radius of the jet, or, more precisely, the distance along the disc where for $\alpha_{\rm out} = 2$ we have $B_{\rm p} = V_{\rm p} = 0$. In Fig. 7 the velocities on the reference line $\alpha = 1$ are plotted in units of V_0, the z-component of the flow speed at the point $(\alpha = 1, \theta = \pi/2)$.

(2) In Figs 8 and 9 an r-self-similar model belonging to case (3) in Table 3 with *parabolic* asymptotic geometry [when $\theta \to 0, (M^2, G^2) \to \infty$] is examined for another set of parameters $(x_i, E_i, C_i, D_i), i = 1, 2$. The Alfvén conical surface is taken now at $\theta_\star = 45°$, where the slope of the square of the Alfvén number is chosen as $p_\star = -1.7$ and the expansion angle $\varphi_\star \approx 75°$.

(3) Finally, in Figs 10 and 11 the r-self-similar model of case (3) in Table 3 gives a *conical* asymptotic geometry for a third set of parameters $(x_i, E_i, C_i, D_i), i = 1, 2$ and $\theta_\star = 65°$, $\varphi_\star = 75°$, $p_\star = -0.5$. Note that now the solution exists only for $\theta > \theta_{\rm min}$ where $\theta_{\rm min} \approx 17.^\circ 5$. When this value of θ is approached, $(M^2, G^2) \to \infty$.

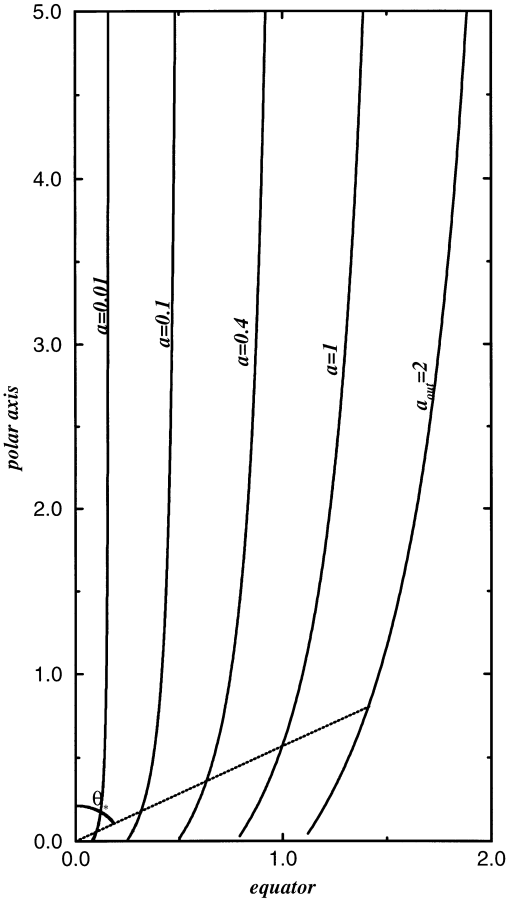

Figure 6. Field and streamlines for the cylindrical r-self-similar model of case (3) from Table 3 and the following set of parameters: $x_1 = -0.9$, $x_2 = -0.6$, $E_1 = -2.142\,1466$, $E_2 = 2.609\,945\,52$, $C_1 = -3.213\,2198$, $C_2 = D_2 = 0$, $D_1 = -160.660\,99$, $\theta_\star = 60°$, $\varphi_\star = 74.^\circ 704\,656$, $p_\star = -1.1$. At the disc level, $V_\phi \propto R^{-1/2}$, while on the poloidal field/streamline $\alpha_{\rm out} = 2$, $B_{\rm p} = V_{\rm p} = 0$.

In all these four possibilities and along a given field/streamline,

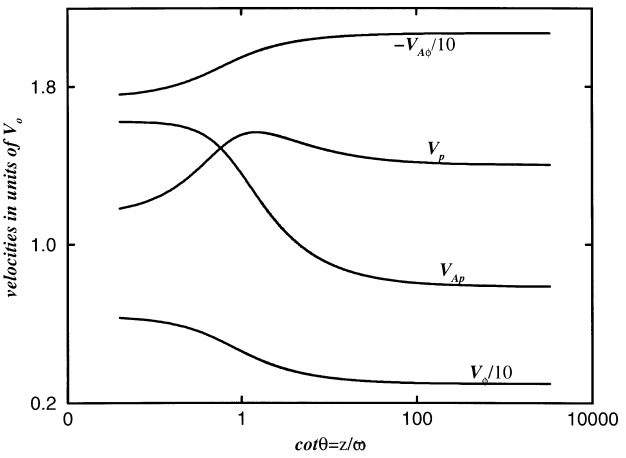

Figure 7. The characteristic velocities of model (3) of Table 3 with cylindrical asymptotics are plotted in units of the z-component of the flow speed V_0 at the point $(\alpha = 1, \theta = \pi/2)$ and for the same parameters as in Fig. 6.

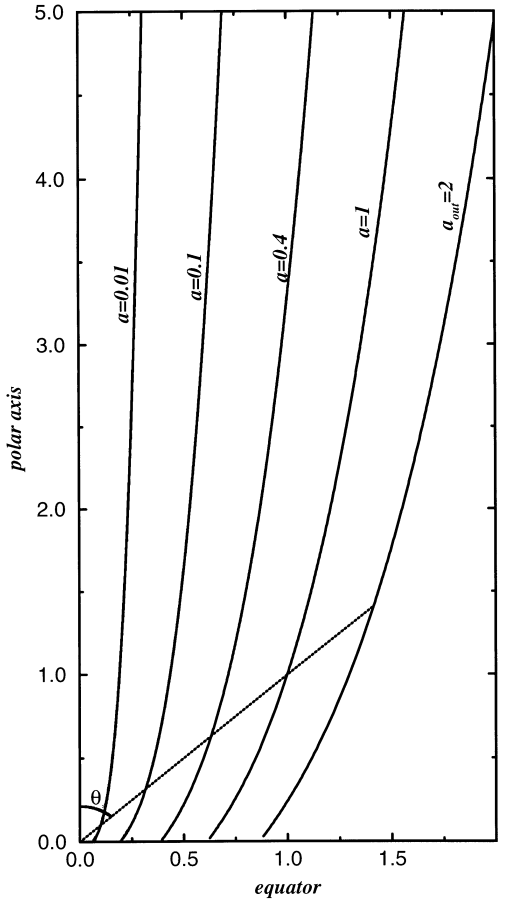

Figure 8. Poloidal field and streamlines for the parabolic r-self-similar model of case (3) from Table 3 and the following set of parameters: $x_1 = -0.9$, $x_2 = -0.6$, $E_1 = -0.825\,2542$, $E_2 = 1.005\,47$, $C_1 = -1.237\,88$, $C_2 = D_2 = 0$, $D_1 = -12.378\,813$, $\theta_\star = 45°$, $\varphi_\star = 75.^\circ 465\,545$, $p_\star = -1.7$. In this case $V_\phi \propto R^{-1/2}$ on the equatorial plane, while on the streamline $\alpha_{\rm out} = 2$, $B_{\rm p} = V_{\rm p} = 0$.

the outflow starts from the equator where $V_\phi \propto R^{-1/2}$ with a low subAlfvénic poloidal speed. This poloidal speed $V_{\rm p}$ crosses the Alfvén conical surface at $\theta_\star$ in all cases. In the cylindrical case of Fig. 7, $V_{\rm p}$ increases rapidly to a uniform value when collimation is achieved. The azimuthal speed V_ϕ, on the other hand, drops with height in all cases, as rotational energy is transformed to poloidal kinetic energy. Finally, the azimuthal Alfvén speed is strongest in the cylindrical case where the toroidal magnetic field is responsible for the ensuing final collimation.

4 SUMMARY

In this paper we have examined a systematic way of constructing exact MHD solutions for plasma flows. The *first* assumption was to consider the ideal plasma MHD equations for time-independent conditions, equations (1) and (2), *without* imposing the extra constraint of the frequently used polytropic assumption. *Secondly*, we confined our attention to axisymmetric situations, in which case the poloidal magnetic and velocity fields can be expressed in terms of the magnetic flux function A while several integrals exist (equations 4–5). In that case, besides A, a second natural variable is the Alfvén Mach number M, equation (3). We denoted by G the cylindrical distance ϖ of a poloidal streamline from the symmetry axis of the system, in units of the cylindrical distance of the Alfvén

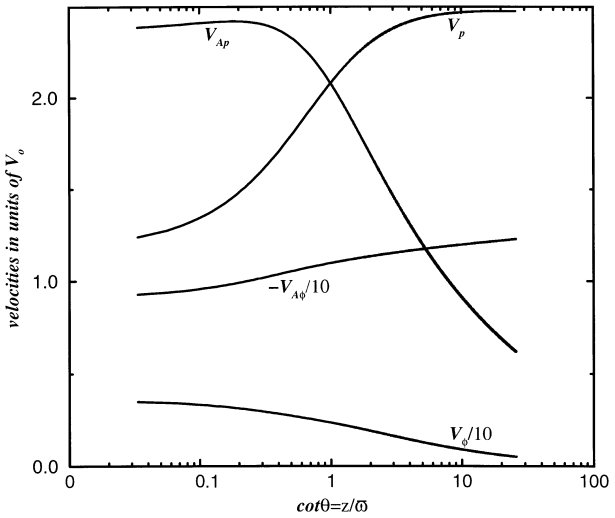

Figure 9. The characteristic velocities of model (3) of Table 3 with paraboloidal asymptotics are plotted in units of the z-component of the flow speed V_0 at the point ($\alpha = 1, \theta = \pi/2$) and for the same parameters as in Fig. 8.

surface from the same axis, ϖ_α. *Thirdly*, we further confined our attention to transAlfvenic outflows in which case the regularization of the azimuthal components in equations (4) and (5) requires that the ratio of the two integrals of the total specific angular momentum in the flow $L(A)$ and corotation frequency $\Omega(A)$ be some function $\alpha(A)$ [as in equation (8)]. By introducing some reference scale ϖ_0 this function α is dimensionless [as in equation (7) where $\varpi_0 \equiv r_\star$]. Apparently (M, α) is a rather convenient set of dimensionless variables for describing all physical quantities in the poloidal plane. For any set of orthogonal curvilinear coordinates suitable for describing axisymmetric problems, we may then convert their poloidal coordinates to (M, α). Examples are spherical coordinates $[r(M,\alpha), \theta(M,\alpha), \phi]$, cylindrical coordinates $[z(M,\alpha), \varpi(M,\alpha), \phi]$, toroidal coordinates $[u(M,\alpha), v(M,\alpha), \phi]$, oblate/prolate spheroidal coordinates $[\xi(M,\alpha), \eta(M,\alpha), \phi]$, paraboloidal coordinates, etc. Then, the distance from the symmetry axis of the outflow is $G(M,\alpha)$. In the present first study we made the simplifying *fourth* assumption that G is independent of α, $G = G(M)$ only. Finally, to re-establish the connection with the geometry of the problem and the particular set of coordinates used, we made our *fifth* and final assumption that $M = M(\chi)$ [and $G = G(\chi)$], where $\chi = r$, or $\chi = \theta$. This leads then to the two broad classes of meridionally and radially self-similar outflows. Needless to say, additional symmetries may in principle be considered, something which may be taken up in another connection (equilibria in tokamak geometries, etc.).

After these five assumptions are well posed, and with the help of a simple theorem, it is possible (i) to unify all existing exact solutions for astrophysical outflows (Tables 1, 2 and 3), and (ii) qualitatively to sketch a few of them. With this method, the system of coupled MHD equations reduces to a set of five ordinary differential equations for the dimensionless jet radius (G), the flow's expansion factor or angle (F or φ), the Alfvén Mach number (M) and the two pressure components (P_1 and P_0). The requirement that the solutions pass through the Alfvén critical point gives a condition relating the values of the expansion function or angle, Alfvén number slope and pressure component at this critical point. The Alfveń regularity conditions, equations (69) and (53) are similar to that discussed by Heyvarts & Norman (1989) and ST94.

As a byproduct of this construction, two representative models

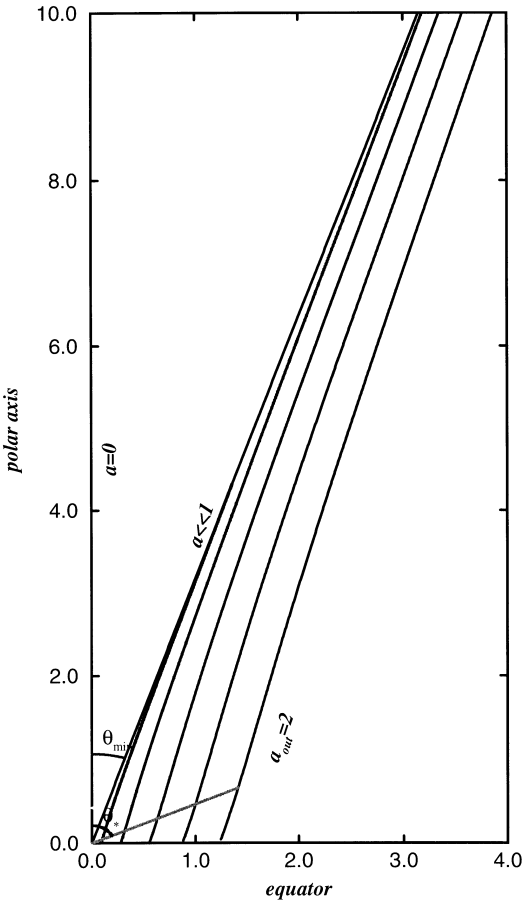

Figure 10. Field and streamlines for the conical r-self-similar model of case (3), Table 3 and the following set of parameters: $x_1 = -0.1, x_2 = 0.01$ and $E_1 = -78.601\,635$, $E_2 = -728.313\,37$, $C_1 = -4.3231$, $C_2 = D_2 = 0$, $D_1 = -43.231$, $\theta_\star = 65°$, $\varphi_\star = 75.°784\,234$, $p_\star = -0.5$. In this case $V_\phi \propto R^{-1/2}$ on the equatorial plane, while on the poloidal field/streamline $\alpha_{\rm out} = 2, B_{\rm p} = V_{\rm p} = 0$. For large distances from the disc all lines with $\alpha > 0$ go asymptotically to the line $\theta = \theta_{\rm min}$.

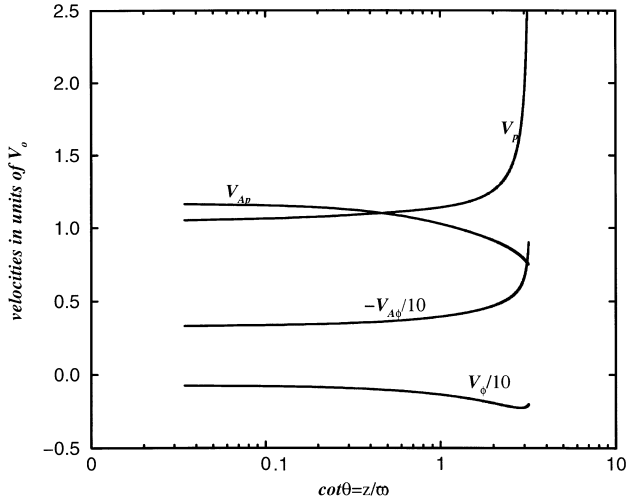

Figure 11. The characteristic velocities of model (3) of Table 3 with conical asymptotic geometry are plotted in units of the z-component of the flow speed at the point $(\alpha = 1, \theta = \pi/2)$, V_0 and for the same parameters as in Fig. 10.

for radially and meridionally self-similar outflows, BP82 and ST94 respectively, have been generalized. In the former case of BP82, it is well known that the cold plasma solution is terminated at a finite height above the disc, while the general case (3) in Table 3 extends all the way to infinity. Also, it is shown that the expressions of the MHD integrals that correspond to the ST94 model are only a special case of case (2) in Table 1.

Having in mind the ubiquitously observed collimated outflows from astrophysical objects, we have paid more attention to the self-consistently derived asymptotic shape of the streamlines. Of the various such asymptotic geometries derived, a prominent class seems to be the cylindrically collimated jet-type solutions, in accordance also with the conclusions of observations (Livio 1997), general theoretical arguments (Heyvaerts & Norman 1989) and recent numerical simulations (Goodson, Winglee & Bohm 1997). Another feature that appeared in the solutions is that cylindrical collimation may or may not be achieved with oscillations in the width of the jet (Vlahakis & Tsinganos 1997). Although in the examples analysed here the amplitude of the oscillations is rather weak and the flow collimates rather smoothly, preliminary results show that cases also exist where it can become rather large and the final radius of the jet can be much smaller than the initial large cylindrical radius and corresponding opening angle. Finally, we should note that the pressure P denotes the total pressure (including gas pressure, Alfvén wave pressure, radiative forces, etc.). For example, the same formalism may also be used in radiation-driven winds.

ACKNOWLEDGMENTS

This research has been supported in part by grant 107526 of the General Secretariat of Research and Technology of Greece. We thank J. Contopoulos, C. Sauty and E. Trussoni for helpful discussions.

REFERENCES

Bardeen J. M., Berger B. K., 1978, ApJ, 221, 105
Biretta T., 1996, in Tsinganos K., ed., Solar and Astrophysical MHD Flows. Kluwer, Dordrecht, p. 357
Blandford R. D., Payne D. G., 1982, MNRAS, 199, 883 (BP82)
Blandford R. D., Rees M. J., 1974, MNRAS, 169, 395
Burderi L., King A. R., 1995, MNRAS, 276, 1141
Burrows C. J., et al., 1995, ApJ, 452, 680
Cao X., 1997, MNRAS, 291, 145
Contopoulos J., Lovelace R. V. E., 1994, ApJ, 429, 139
Crane P., Vernet J., 1997, ApJ, 486, L91
Feldman W. C., Phillips J. L., Barraclough B. L., Hammond C. M. 1996, in Tsinganos K., ed., Solar and Astrophysical MHD Flows. Kluwer, Dordrecht, p. 265
Ferrari A., Massaglia S., Bodo G., Rossi P., 1996, in Tsinganos K., ed., Solar and Astrophysical MHD Flows. Kluwer, Dordrecht, p. 607
Ferreira J., 1997, A&A, 319, 340
Ferreira J., Pelletier G., 1995, A&A, 295, 807
Goodson A. P., Winglee R. M., Bohm K. H., 1997, ApJ, 489, 199
Heyvaerts J., Norman C. A., 1989, ApJ, 347, 1055
Kafatos M., 1996, in Tsinganos K., ed., Solar and Astrophysical MHD Flows. Kluwer, Dordrecht, p. 585
Konigl A., 1989, ApJ, 342, 208
Li Z.-Y., 1995, ApJ, 444, 848
Lima J., Tsinganos K., Priest E., 1996, Astrophys. Lett. Commun., 34, 281
Livio M., 1997, in Wickramasinghe D. T., Ferrario L., Bicknel G. V., eds, ASP Conf. Proc. Vol. 121, Accretion Phenomena and Related Outflows. Astron. Soc. Pac., San Francisco, p. 845

Mirabel I. F., Rodriguez L. F., 1996, in Tsinganos K., ed., Solar and Astrophysical MHD Flows. Kluwer, Dordrecht, p. 683
Parker E. N. 1958, ApJ, 128, 664
Ray T. P., 1996, in Tsinganos K., ed., Solar and Astrophysical MHD Flows. Kluwer, Dordrecht, p. 539
Sauty C., Tsinganos K., 1994, A&A, 287, 893 (ST94)
Trussoni E., Tsinganos K. E., Sauty C., 1997, A&A, 325, 1099
Tsinganos K. C., 1982, ApJ, 252, 775
Tsinganos K., Sauty C., Surlantzis G., Trussoni E., Contopoulos J., 1996, MNRAS, 283, 811
Vlahakis N., Tsinganos K., 1997, MNRAS, 292, 591

APPENDIX A FUNCTIONS OF *R*

$$F = 2 - R\frac{G^{2'}}{G^2} \equiv \frac{\partial \ln \alpha(R,\theta)}{\partial \ln R}\,. \tag{A1}$$

$$f_1 = -\frac{1}{G^4}\,, \tag{A2}$$

$$f_2 = -\frac{F^2-4}{4G^2R^2}\,, \tag{A3}$$

$$f_3 = -\frac{1}{G^2}\left(\frac{1-G^2}{1-M^2}\right)^2, \tag{A4}$$

$$f_4 = \frac{F}{2RG^2}M^{2'} - \frac{1-M^2}{2RG^2}F' - \frac{\left(1-M^2\right)F(F-2)}{4R^2G^2}\,, \tag{A5}$$

so

$$F' = \frac{F}{1-M^2}M^{2'} - \frac{F(F-2)}{2R} - \frac{2RG^2}{1-M^2}f_4\,, \tag{A6}$$

$$f_5 = \frac{G^4-M^2}{G^2M^2\left(1-M^2\right)}\,, \tag{A7}$$

$$f_6 = -\frac{2}{G^4}M^{2'} + \frac{2\left(1-M^2\right)(F-2)}{RG^4}\,, \tag{A8}$$

$$f_7 = \frac{2}{R^2G^2}M^{2'} - \frac{\left(1-M^2\right)(F-2)(F+4)}{2R^3G^2} - \frac{F}{R}f_4\,, \tag{A9}$$

$$f_8 = -\frac{F-2}{R}f_5\,, \tag{A10}$$

$$f_9 = -\frac{\nu^2}{R^2M^2}\,. \tag{A11}$$

APPENDIX B FUNCTIONS OF θ

$$H = 2 - \frac{G^{2'}}{G^2} \equiv \frac{\partial \ln \alpha(R,\theta)}{\partial \ln \sin\theta}\,, \tag{B1}$$

$$H = -2\frac{\sin\theta\sin(\varphi+\theta)}{\cos\theta\cos(\varphi+\theta)} = 2 - 2\frac{\cos\varphi}{\cos\theta\cos(\varphi+\theta)}\,, \tag{B2}$$

where the expansion angle φ is the angle between the line and the equatorial plane, which is a function of θ.

$$\frac{\mathrm{d}G^2}{\mathrm{d}\theta} = \frac{2G^2\cos\varphi}{\sin\theta\cos(\varphi+\theta)}\,, \tag{B3}$$

$$h_1 = -\frac{\left(\sin^2\theta + \cos^2\theta\frac{H^2}{4}\right)}{G^4} = -\frac{\sin^2\theta}{G^4\cos^2(\varphi+\theta)}\,, \tag{B4}$$

$$h_2 = -\frac{1}{G^2}\left(\frac{1-G^2}{1-M^2}\right)^2, \tag{B5}$$

$$h_3 = \frac{G^4-M^2}{M^2G^2\left(1-M^2\right)}\,, \tag{B6}$$

$$h_4 = -\frac{\sin\theta}{GM^2}\,, \tag{B7}$$

$$h_5 = -\frac{\cos^2\theta}{2G^4}\Big\{\left[H\left(1-M^2\right)\right]' + (H-2)\left(1-M^2\right)\left(H-\tan^2\theta\right)\Big\}\,, \tag{B8}$$

or

$$h_5 = \frac{1-M^2}{G^4}\frac{\sin^2\theta}{\cos^2(\varphi+\theta)}\frac{\mathrm{d}\varphi}{\mathrm{d}\theta} - \frac{\sin^2\theta\sin(\varphi+\theta)}{G^4\cos(\varphi+\theta)}\frac{\mathrm{d}M^2}{\mathrm{d}\theta} - \frac{1-M^2}{G^4}\frac{\sin\theta\cos\varphi\sin(\varphi+\theta)}{\cos^2(\varphi+\theta)}\,, \tag{B9}$$

so

$$\frac{\mathrm{d}\varphi}{\mathrm{d}\theta} = \frac{\sin(\varphi+\theta)\cos(\varphi+\theta)}{1-M^2}\frac{\mathrm{d}M^2}{\mathrm{d}\theta} + \frac{\sin(\varphi+\theta)\cos\varphi}{\sin\theta} + \frac{\cos^2(\varphi+\theta)}{\sin^2\theta}\frac{G^4}{1-M^2}h_5\,. \tag{B10}$$

This paper has been typeset from a TEX/LATEX file prepared by the author.